

ELECTRON AND PROTON BEAM DIAGNOSTICS WITH SYNCHROTRON RADIATION

A. Hofmann

CERN, 1211 Geneva 23, Switzerland.

Summary

Synchrotron radiation is widely used to measure the cross-section of the electron beams. Large photon fluxes within a convenient part of the spectrum are radiated by the electrons in the bending magnets. To obtain sufficient intensities of visible light from high energy protons, there are special magnets needed which alter the normal spectral distribution of the radiation. The resolution of the cross-section measurement is limited by diffraction. This limit can be improved by working with a short wave length or by using the radiation from short magnets.

1. Introduction

Synchrotron radiation is a convenient tool to measure the cross section of electron and recently also of proton beams. For technical reasons this observation is done preferably with visible light. In the case of electrons this implies the use of the lower energy part of the spectrum emitted in the bending magnets. For protons with energies of a few hundred GeV sufficient intensity of visible light can only be obtained with special magnets. The synchrotron radiation represents a rather unusual optical source. It has a small natural opening angle and a relatively large extension in the direction of emission and the radiation emitted in long bending magnets sweeps along the plane of the particle orbit. The optical geometry involved in forming an image of the beam cross section is rather complicated and has been discussed extensively^{1,2}. The present investigation concentrates on the principal properties of the radiation emitted in different kinds of magnets and the resulting consequences for beam observation.

2. Some general properties of synchrotron radiation

2.1 Total radiated power

Electromagnetic radiation is emitted from accelerated electrical charges. The particular properties of synchrotron radiation are caused by the ultra-relativistic motion of the charged particle. The total instantaneous power P radiated by such a particle with rest mass m_0 , charge e and energy E going through a transverse magnetic field B is³

$$P = \frac{2}{3} \frac{r_0 c^3 e^2 B^2 E^2}{(m_0 c)^3} \quad (1)$$

where $r_0 = e^2 / (4\pi\epsilon_0 m_0 c^2)$ is the classical radius of the particle. This expression (1) is generally valid for any practical magnet if the particle moves in vacuum and the effects of the surroundings on the radiation can be ignored.

2.2 Qualitative properties of the radiation from long magnets

The Lorentz transformation of the approximately uniform distribution in a frame F' moving (for an instant) with the electron into the laboratory frame F, results in a sharply peaked angular distribution of the radiation with a typical opening angle $1/\gamma$. This has some consequences for the observed spectrum. The particle can be 'seen' by an observer only while it covers a part of the trajectory of approximate length $L \approx 2\rho/\gamma$,

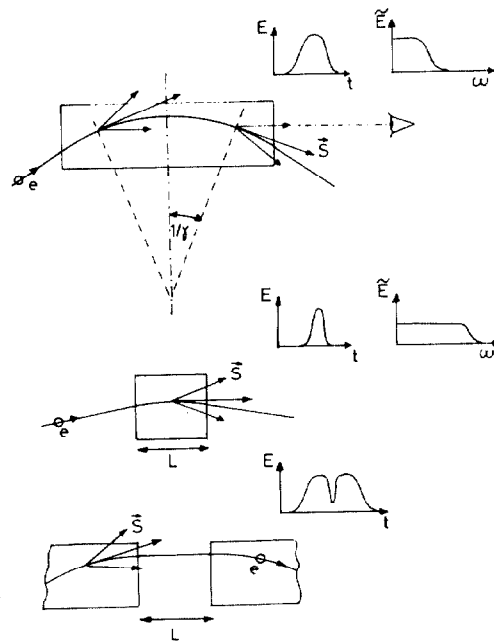


Fig. 1 : Estimation of the spectrum of the synchrotron radiation from long and short magnets

where ρ is the bending radius⁴. The duration Δt of the received radiation pulse is equal to the difference of the arrival times of photons emitted from the two extreme points of the observed trajectory; Fig. 1.

$$\Delta t = t_e - t_\gamma \approx \frac{2\rho}{\beta\gamma c} - 2 \sin\left(\frac{1}{\gamma}\right) \frac{\rho}{c} \approx \frac{\rho}{c\gamma^3}$$

This gives a typical frequency of the radiated spectrum

$$\omega_{typ} \approx 2\pi \frac{c\gamma^3}{\rho}$$

2.3 Qualitative properties of the radiation from short weak magnets

If the magnet is short and relatively weak such that the occurring bending angle is smaller than $1/\gamma$, the observed radiation pulse becomes shorter, Fig. 1.

$$\Delta t = t_e - t_\gamma \approx \frac{L}{c} \cdot \frac{1}{2\gamma^2}$$

and the resulting typical frequency

$$\omega_{typ} \text{ (short magnet)} \approx 2\pi \frac{2\gamma^2 c}{L}$$

If the magnet is very short ($L \ll \rho/\gamma$) the high frequency part of the spectrum is enhanced compared to the spectrum from long magnets; the total power, however, is still given by (1). For practical magnets this situation can easily be realized for protons but less likely for electrons. If the short magnet radiation is observed under an angle θ with respect to the particle motion, the typical frequency becomes

$$\omega_{typ} \approx 2\pi \frac{2\gamma^2 c}{L} \frac{1}{1+\gamma^2\theta^2} \quad (2)$$

A similar spectrum is obtained for the radiation emitted in the neighbourhood of a sharp depression of the magnetic field which usually occurs between two bending magnets; Fig. 1.

The opening angle of the short magnet radiation is increased compared to the normal radiation. Taking (2) for $\omega \ll \omega_{typ}$ one finds for the opening angle

$$\theta \sim \sqrt{\frac{2\lambda}{L}}$$

This large opening angle can improve the resolution of beam observation with synchrotron radiation⁵.

3. Radiation from long homogeneous magnets

Usually one observes the synchrotron radiation emitted in the long, homogeneous bending magnets. The detailed properties of this radiation have been derived by D. Ivanenko and A.A. Sokolov⁶ and by J. Schwinger⁷ and can be found in text books^{4,8}. Since the beam of radiation sweeps along the plane of the particle orbit, the angular distribution in this direction (angle φ in Fig. 2) cannot, in most practical cases, be observed. It is therefore convenient to average over the horizontal angle φ and give the distribution with respect to the angle ψ perpendicular to the orbit plane; fig. 2. The power radiated per unit solid angle

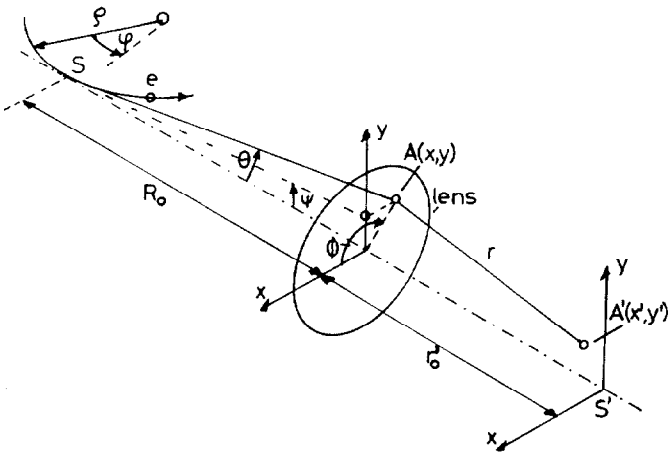


Fig. 2 : Geometry of the beam cross section measurement ($d\varphi d\psi$) and frequency interval is $\frac{d^3P}{d\varphi d\psi d\omega} =$

$$\left(\frac{3}{2\pi}\right)^3 \frac{P_0 \gamma}{\omega_c} \frac{\xi^2}{1+\gamma^2 \psi^2} \left[K_{2/3}^2(\xi) + \frac{\gamma^2 \psi^2}{1+\gamma^2 \psi^2} K_{1/3}^2(\xi) \right] \quad (3)$$

with $\omega_c = \epsilon_c / \hbar = \frac{3}{2} \frac{c\gamma^3}{\rho} =$ critical frequency (4)

and $\xi = \frac{\omega}{2\omega_c} \left(1 + \gamma^2 \psi^2 \right)^{3/2}$

Here P_0 is the total radiated power (1) and $K_{2/3}(\xi)$ and $K_{1/3}(\xi)$ are modified Bessel functions. The first term in the parentheses refers to the direction of the polarization with the electrical vector being in the plane of the orbit, also called σ -mode. The second term refers to the vertical polarization or π -mode. The angular distribution of the two modes is shown in Fig. 3 after integration over all frequencies and in Fig. 8 for a particular frequency $\omega = 0.01 \omega_c$. The typical opening angle of the total distribution is

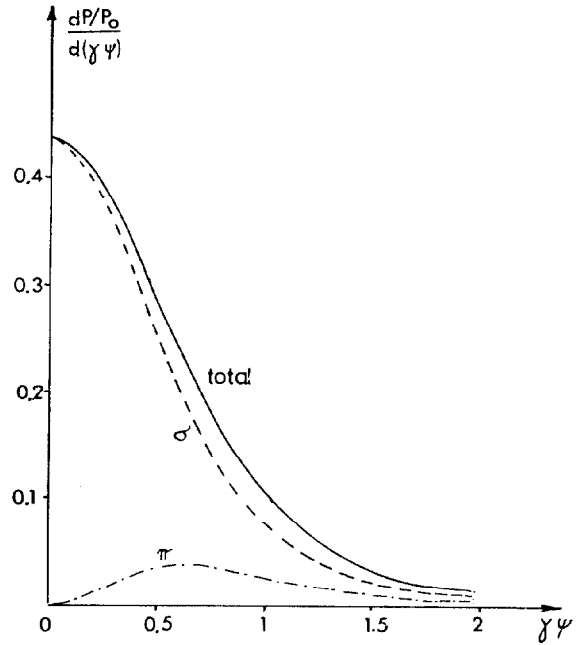


Fig. 3 : Angular distribution of the integrated spectrum from long magnets

$$\psi_{typ} \approx \frac{1}{\gamma} \left(\frac{\omega_c}{\omega} \right)^{1/3} \quad (5)$$

The spectrum of the total radiation is obtained by integrating (3) over all angles

$$\frac{dP}{d\omega} = \frac{P_0}{\omega_c} S\left(\frac{\omega}{\omega_c}\right);$$

$$S\left(\frac{\omega}{\omega_c}\right) = \frac{9\sqrt{3}}{8\pi} \left(\frac{\omega}{\omega_c}\right) \int_{\omega/\omega_c}^{\infty} K_{5/3}\left(\frac{\omega}{\omega_c}\right) d\left(\frac{\omega}{\omega_c}\right) \quad (6)$$

This spectrum is shown in Fig. 4.

For electrons the observed frequency is well below the critical frequency. In this case, the spectrum can conveniently be approximated by⁹

$$S\left(\frac{\omega}{\omega_c}\right) \approx 1.34 \left(\omega/\omega_c\right)^{1/3} \text{ for } \omega \ll \omega_c$$

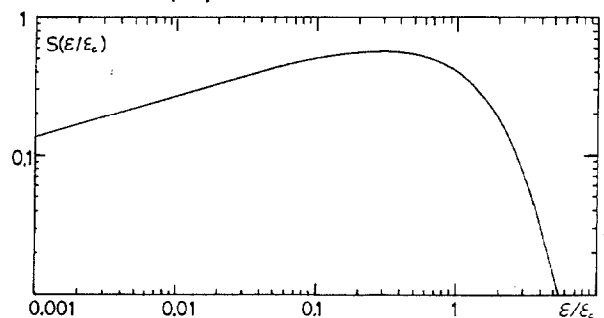


Fig. 4 : The function $S(\epsilon/\epsilon_0)$ describing the total synchrotron radiation spectrum.

4. Radiation from undulators and short weak magnets

An undulator is a periodic structure designed to produce quasi monochromatic radiation¹⁰. In such a periodic magnetic field

$$B = B_0 \sin\left(\frac{2\pi}{\lambda_u} z\right)$$

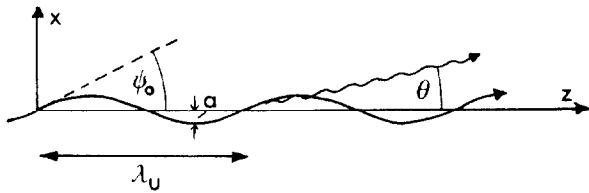


Fig. 5 : Particle trajectory in an undulator

the particle trajectory is approximately (Fig. 5)

$$x = a \sin \left(\frac{2\pi}{\lambda_u} z \right) = \psi_0 \frac{\lambda_u}{2\pi} \sin \left(\frac{2\pi}{\lambda_u} z \right)$$

with λ_u = period length, a = amplitude and ψ_0 maximum angle between the electron trajectory and the z-axis;

$$\psi_0 = \frac{eB_0 \lambda_u c}{2\pi m_0 c^2 \gamma} = \frac{K}{\gamma}$$

In the following, it is assumed that the transverse motion is non-relativistic, therefore $\psi_0 \ll 1/\gamma$ and $K \ll 1$. In a frame F' moving with the drift velocity of the particle, the motion is a simple harmonic oscillation emitting the well known dipole radiation. Moving back into the laboratory frame, one obtains the angular distribution of the radiation of a weak field undulator of length L_u , ($L_u \gg \lambda_u$)^{10,11,12}.

$$\frac{dP_1}{d\Omega} = \frac{3P_1 \gamma^2}{\pi} \left(1 - \gamma^2 \theta^2 \cos 2\phi \right)^2 \left| \frac{dP}{d\Omega} = \frac{3P_1 \gamma^2}{\pi} (\gamma\theta)^4 \sin^2 2\phi \right. \quad (7)$$

where P_1 is the total power radiated by one particle while going through the undulator;

$$\kappa = (1 + \gamma^2 \theta^2)^5, \quad P_1 = \frac{r_0 e^2 c^3 B_0^2 \gamma^2}{3 m_0 c^2}$$

and $d\Omega = \sin \theta d\theta d\phi$ is the solid angle according to Fig. 2. The frequency radiated at a fixed angle θ is monochromatic for an infinite number of periods

$$\omega_1 \approx \frac{2\pi c}{\lambda_u} 2\gamma^2 \frac{1}{1 + \gamma^2 \theta^2} = \omega_{10} \frac{1}{1 + \gamma^2 \theta^2} \quad (8)$$

Integrating over all angles gives the total spectrum

$$\frac{dP}{d\omega} = \frac{3P_1}{\omega_{10}} \left(\frac{\omega}{\omega_{10}} \right) \left(1 - 2 \frac{\omega}{\omega_{10}} + 2 \left(\frac{\omega}{\omega_{10}} \right)^2 \right) \quad (9)$$

shown in Fig. 6. The angular distribution of the radiation is shown in Fig. 7 for $\phi = 0$ and $\phi = \pi/2$; at these angles θ the π -mode vanishes.

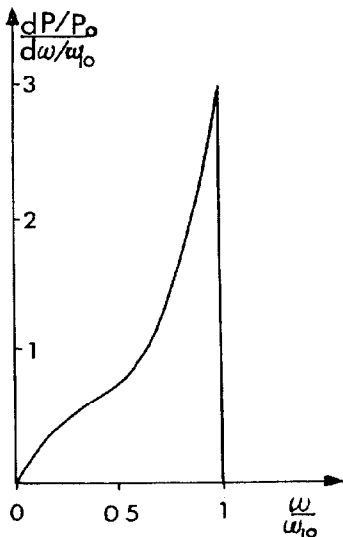


Fig. 6: Total spectrum from a weak field undulator

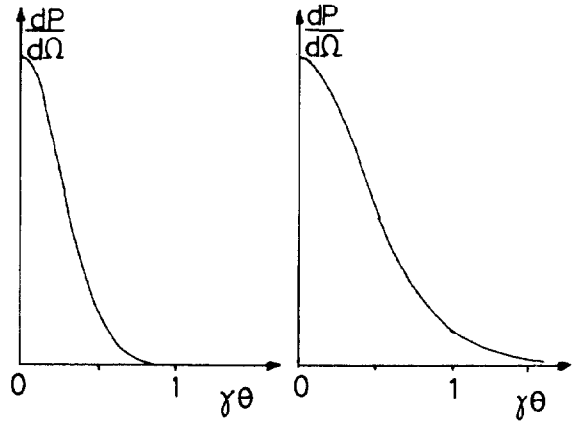


Fig. 7 : Angular distribution of the integrated spectrum from a weak field undulator; left: $\phi = 0$, right: $\phi = \pi/2$.

According to (8) the undulator spectrum can cover rather high frequencies if the period length λ_u is short. This led to the suggestion of using undulators to obtain visible radiation from protons^{13,14}.

It is always assumed here that the undulator is weak, that is $K \ll 1$. The spectrum of a strong field undulator contains higher harmonics and is much more complicated¹⁵.

The radiation from short weak magnets can be understood as a generalization of undulator radiation. A magnet is considered to be short and weak if the maximum deflection angle is small compared to $1/\gamma$ such that the transverse motion is always non-relativistic. In this case, the magnetic field can be Fourier analyzed, in other words, decomposed into undulator fields of different period length λ_u . The spectrum and angular distribution of each component is known and the total spectrum can be obtained by summation¹⁶.

5. Optical resolution of the beam cross section measurement

The optical resolution of the beam cross section measurement is limited by diffraction and depth of field. Since the horizontal beam dimension is usually larger than the vertical one, only the vertical resolution is of concern.

The measurement of the beam cross section is usually done with a set-up similar to the one outlined in Fig. 2. A lens forms an image S' of a source S . To observe the radiation from long magnets the horizontal aperture of the lens should be matched to the natural opening angle of the radiation². This improves the depth of field problems and the definition of the source point.

The small opening angle θ of the radiation leads to a resolution d limited by diffraction analogue to a lens with limited aperture $d \approx \frac{\lambda}{\theta}$

For the radiation from long magnets one gets from (5) and (4) for this resolution^{17,18}

$$d = f_r \lambda \gamma \left(\frac{\lambda_c}{\lambda} \right)^{1/3} = f_r \left(\frac{4\pi}{3} \right)^{1/3} \lambda^{2/3} \gamma^{1/3} \quad (10)$$

with f_r being a form factor of order unity to be discussed later.

The resolution due to the depth of field depends on the length L of the observed orbit and the opening angle θ ; d (depth of field) $\approx L\theta/4$.

For short magnets and undulators L is fixed, the resolution due to depth of field gets worse with increasing angle θ while the resolution due to diffraction improves. Assuming no artificial acceptance limitation of lens, the relevant opening angle θ is related through (2) and (8) to the observed wave length λ . The resolution can be optimized by choosing the latter¹⁹.

In the case of the radiation from long magnets the observed orbit length depends on the natural horizontal opening angle and hence on the observed wave length. The resolution due to depth of field is approximately proportional but somewhat better than the resolution due to diffraction.

The following part is restricted to the problem of diffraction although the effects of the depth of field have to be taken into account in many practical cases. We consider first the case of a single electron which emits in one traversal a coherent wave. The angular distribution of the radiation creates an amplitude distribution $(A(x,y))$ of the wave in the plane of the lens in Fig. 2. This amplitude is defined such that the power distribution is proportional to $|A^2|$. According to Huygen's principle, each point at the lens represents a source of a secondary wave with amplitude $A(x,y)$ which produces a diffraction pattern with amplitude $A'(x',y')$ in the image plane. Since the angle is very small the diffraction is of the Fraunhofer type where the amplitude $A'(x',y')$ of the diffraction is related to the amplitude $A(x,y)$ at the lens by a two dimensional Fourier transformation²⁰. This relation holds for both polarization modes independently, and the total intensity distribution of the diffraction pattern is the sum of the σ - and π -mode intensity. A detailed description of this procedure and its applications to the different cases of synchrotron radiation is given in refs 20 and 21.

As an illustrating example the case of ordinary synchrotron radiation from long magnets far below the critical energy ($\epsilon = 0.01 \epsilon_c$) is shown in Fig. 8. For this radiation the distribution (3) is averaged over the horizontal angles and the two dimensional Fourier transformations can in first approximation be replaced by a one dimensional one involving only the coordinate $y = \psi \cdot R_0$. On the left of Fig. 8 the unnormalized intensity $|A(y)|^2$ at the lens is shown for both polarization modes. The right hand side shows the intensity of the diffraction pattern obtained by Fourier transformation. It represents the response function of the measurement to a point source (neglecting depth of field and other effects). The figure clearly shows that a modest improvement of the resolution can be obtained by selecting only the σ -mode

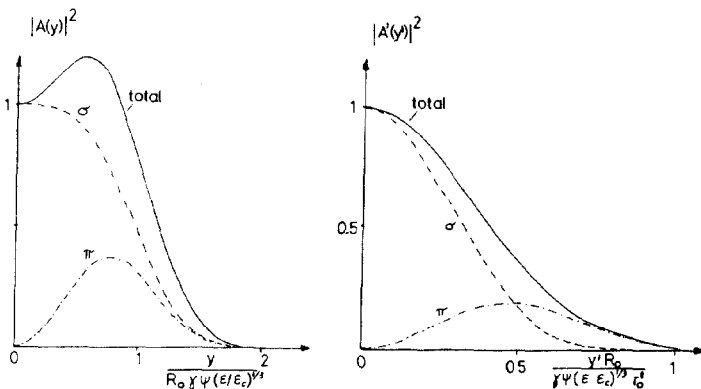


Fig. 8 : left: angular distribution of the synchrotron radiation intensity for $\omega = 0.01 \omega_c$ right: intensity of the corresponding interference pattern.

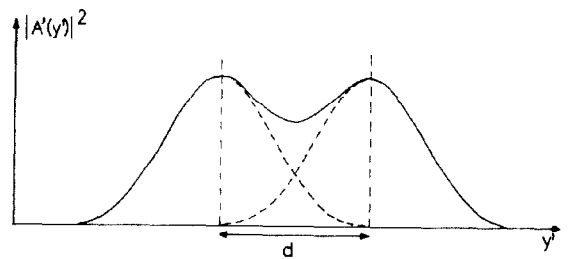


Fig. 9 : Intensity of the interference pattern from 2 point sources separated by d .

of the polarization. In Fig. 9 the response to two points, separated by the distance d is shown. The obtainable resolution depends on the contrast necessary for separations. Assuming a depression of the diffraction pattern intensity down to 2/3 between the two peaks in Fig. 9 is sufficient, one obtains for the form factor in (10) $f_r \sim 0.5$.

In the case of many particles, the radiation is usually incoherent and the waves emitted by different particles do not interfere on average. The intensity of the image pattern is the sum of the intensities due to individual particles.

6. Application and examples

For electrons the radiation from the long bending magnets is commonly used and the spectral angular distribution is thereby determined. The photon energies used for observation is usually far below the critical energy. The resolution in the visible region can be rather limited for very high energy electrons. The expression (10) suggests the use of shorter wave lengths. In the example shown in Figs. 10 and 11, x-rays with $\lambda \sim 0.5 \text{ \AA}$ were used¹⁷. An image of the beam cross section was formed by means of a pinhole of

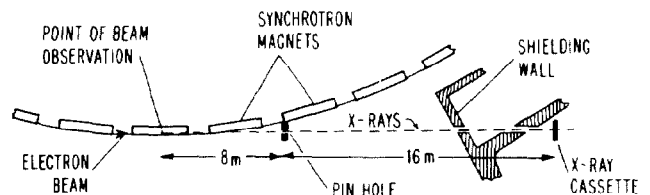


Fig. 10: Set-up for beam size measurement using x-rays; ref.17

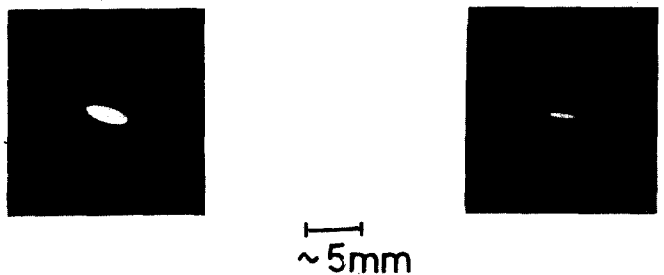


Fig. 11: Beam image formed by x-rays for 2 different amounts of coupling; ref.17

0.07 mm diameter. The final resolution was about 0.1 mm determined mainly by the finite pinhole size. The use of short magnets for electrons has been suggested to improve the resolution in the visible region⁵. It could avoid the technical complications of x-rays and UV-optics. For protons of a few hundred GeV energy, short magnets or undulators are necessary to obtain sufficient intensities in the visible region^{13,14}. The undulator can be designed such that the peak of the spectrum lies in the visible region for a given proton energy and with filter, the wave length giving the best resolution can be selected. The use of the radiation emitted in the neighbourhood of a field depression is shown in Figs. 12 - 14 for the example of the CERN SPS^{22,23}. The field shape $B(s)$ between two bending magnets is shown in Fig. 12. The calculated

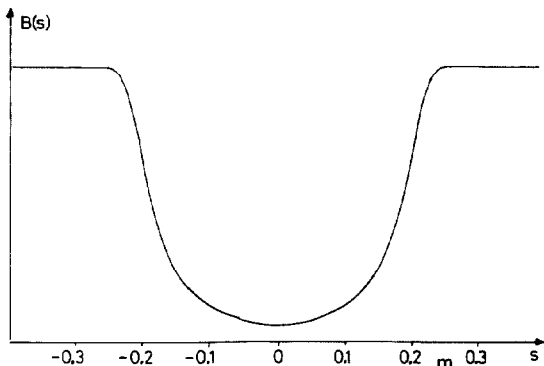


Fig. 12: Depression of the magnetic field between two SPS magnets; ref.22

spectrum on the axis ($\theta=0$) is shown in Fig. 13. It shows peaks due to interference between waves originating at the two sharp edges of $B(s)$.

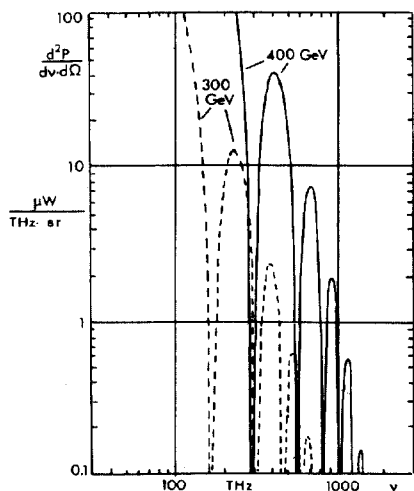


Fig. 13: Computed power spectrum per unit solid angle on the axis $\theta=0$ for a proton beam current of 100 mA in the SPS; ref.22

In Fig. 14, the calculated spectrum integrated over angles is shown together with 'normal' radiation from the long bending magnets and the sensitivity of the photomultiplier. Although the total power radiated in the visible region is less than 1nW excellent pictures of the beam cross section could be obtained²³.

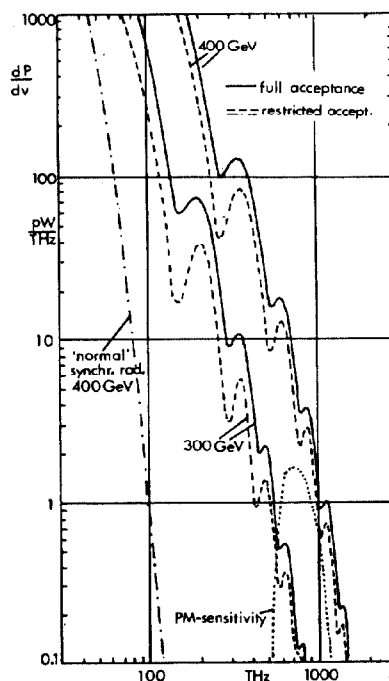


Fig. 14: Computed power spectrum integrated over angles and photomultiplier sensitivity; ref.22

Acknowledgements

I would like to thank R. Coisson and F. Méot for many fruitful discussions and clarifications.

References

- 1 G.K. Green, BNL 50592, Vol. 2 (1975).
- 2 A. Sabresky; Particle Accel.5 (1973) 199.
- 3 A.H. Liénard, L'Eclairage Electr. 16 (1898), 5.
- 4 J.D. Jackson, Classical Electrodynamics, (Wiley, 1962), p. 464.
- 5 K.W. Robinson, Private Communication, 1967.
- 6 D.D. Ivanenko, A.A. Sokolov, Doklady Akad. Nauk (SSSR), 59 (1948), 1551.
- 7 J. Schwinger, Phys. Rev. 75 (1949), 1912.
- 8 A.A. Sokolov and I.M. Ternov, Synchrotron Radiation (Pergamon Press, 1966).
- 9 M. Sands, SLAC 121 (1970).
- 10 H. Motz, J. Appl. Phys. 22 (1976), 177.
- 11 A. Hofmann, Nucl. Instr. Meth., 152 (1978), 17.
- 12 A.N. Didenko et al. JETP 49 (6) (1979), 973.
- 13 R. Coisson, IEEE Trans. on Nucl. Sci., NS-24, no.3 (1977), 1681.
- 14 D.F. Alferov, E.G. Bessonov, 10th Int. Conf. on High Energy Accel., Serpukov 1977, Vol. 2, p. 387.
- 15 D.F. Alferov, Ya. A. Basmakov, E.G. Bessonov, Synchrotron Radiation, Lebedev Phys. Inst. Series 80, ed. N.G. Basov, New York Consultants Bureau (1976), p. 97.
- 16 R. Coisson, Phys. Rev. A, Vol. 20 (1979), 524.
- 17 A. Hofmann, K.W. Robinson, IEEE Trans. Nucl. Sci. (1973), 937.
- 18 A.M. Kondratenko, Novosibirsk, Private Communication
- 19 F. Méot, Private Communication.
- 20 F. Méot, SPS Informal Note, 28.01.80.
- 21 A. Hofmann, F. Méot. CERN-SPS (1981).
- 22 R. Bossart et al., Nucl. Instr. Meth. 164, (1979), 375.
- 23 R. Bossart et al., 11th Int. Conf. on High Energy Accel., CERN 1980, p. 470.